Supplementary Information

A PtPdCoCuNi High-Entropy Alloy Nanocatalyst for the Hydrogenation of Nitrobenzene

Fagui Lu[a], Kuan Lu[b], Gui Zhao[a], Song Zhou[c], Bowen He[a], Yixiao Zhang[a], Jian Xu[c], Yongwang Li[c], Xi Liu*[ad] and Liwei Chen*[ad]

[a] School of Chemistry and Chemical Engineering, In-situ Center for Physical Sciences, Frontiers Science Center for Transformative Molecules, Shanghai Jiao Tong University, Shanghai 200240, China

[b] State Key Laboratory of Coal Conversion, Institute of Coal Chemistry, Chinese Academy of Sciences, Taiyuan 030001, China

[c] SynCat@Beijing Synfuels China Technology Co. Ltd., Beijing 101407, China

[d] Shanghai Jiao Tong University, China Shanghai Electrochemical Energy Device Research Center (SEED), Shanghai 200240, China

Chemicals

SiO_2 was bought from Alfa Aesar. Ethylene glycol (AR), anhydrous alcohol (AR), and cyclohexane (AR) were all purchased from Sinopharm Chemical Reagent Co., Ltd. Nickel (II) acetylacetonate ($Ni(acac)_2$, AR), platinum (II) acetylacetonate ($Pt(acac)_2$, RG), oleylamine (RG), and poly(vinyl pyrrolidone) (PVP, average MW = 40000) were procured from Adamas-Beta. Cupric (II) acetylacetonate ($Cu(acac)_2$, 97%), sodium citrate (AR), potassium bromide (KBr, AR), and nitrobenzene (AR) were all obtained from Aladdin Industrial Co., Ltd. Cobalt (II) acetylacetonate ($Co(acac)_2$, 99%) and palladium (II) acetylacetonate ($Pd(acac)_2$, 99%) were supplied by Macklin. All the chemicals were used as obtained without further purification.

Synthesis of PtPdCoCuNi Nanoparticles

To prepare the PtPdCoCuNi nanoparticles, 4.0 mg $Pt(acac)_2$, 3.0 mg $Pd(acac)_2$, 2.6 mg $Co(acac)_2$, 2.7 mg $Cu(acac)_2$, 2.7 mg $Ni(acac)_2$, 50 mg KBr, 80 mg sodium citrate,

and 100 mg PVP were all dissolved in 10 mL ethylene glycol with stirring at 70 °C. The resulting homogeneous solution was transferred to a Teflon-lined steel autoclave. The sealed vessel was then heated at 200 °C for 12 h in the oven before it was cooled to room temperature. The black products were obtained by centrifugation and washed with anhydrous ethanol. Then 10 mL ethanol, 1 mL oleylamine, and 8 mL cyclohexane were added to the resulting products. The mixture was refluxed at 70 °C for 12 h. The PtPdCoCuNi nanoparticles were obtained by centrifugation and subsequently washed with mixture of ethanol-cyclohexane (1:1). The obtained PtPdCoCuNi nanoparticles were dispersed in 10 mL cyclohexane for further experiments. For the syntheses of Pt, Pd, Co, Cu, Ni, PtPd, PtPdCo, PtPdCoCu, $PtPd(CoCuNi)_{1.5}$, $PtPd(CoCuNi)_2$, and $PtPd(CoCuNi)_4$ nanoparticles, all of the conditions were similar to those of PtPdCoCuNi, except for the amounts and the kinds of metal precursors. The total metal precursors were kept to 0.05 mmol.

Synthesis of PtPdCoCuNi/SiO_2 catalyst

10 mL PtPdCoCuNi (theoretical amount of 4.8 mg) cyclohexane suspension was dispersed in 20 mL cyclohexane under sonication. The obtained nanoparticle dispersion was added dropwise to SiO_2 (240 mg) cyclohexane (10 mL) suspension under stirring. The product was collected by centrifugation and dried at 60 °C for 12 h. The theoretical metal loading was controlled at 2.0 wt%. The obtained sample was heated in a tube furnace at 160 °C for 5 h under H_2 flow (50 mL/min). The resulting sample was denoted as PtPdCoCuNi/SiO_2. The Pt/SiO_2, Pd/SiO_2, Co/SiO_2, Cu/SiO_2, Ni/SiO_2, PtPd/SiO_2, PtPdCo/SiO_2, PtPdCoCu/SiO_2, $PtPd(CoCuNi)_{1.5}/SiO_2$, $PtPd(CoCuNi)_2/SiO_2$, and $PtPd(CoCuNi)_4/SiO_2$ catalysts were prepared by the same process.

Materials characterization

BET surface area and pore distribution were tested on a micromeritics ASAP 2420 instrument. X-ray diffraction (XRD) patterns were collected on a Bruker D8 Advance diffractometer using Cu Kα radiation operating at 40 kV and 40 mA. Transmission electron microscopy (TEM) images were obtained using JEOL JEM 2100 at 200 kV with a thermionic LaB_6 source. Scanning transmission electron microscopy (STEM)

and energy dispersive X-ray spectroscopy (EDS) mapping were acquired with Hitachi HF5000 at 200 kV using a cold field emission gun. X-ray photoelectron spectroscopy (XPS) analyses were performed on a Kratos Axis Ultra DLD using Al Kα as the excitation source. The elemental analyses were determined with inductively coupled plasma atomic emission spectroscopy (ICP–AES) on a PerkinElmer Avio 500 instrument. ^{1}H NMR and ^{13}C NMR spectra were recorded on a Bruker 500 Nuclear Magnetic Resonance spectrometer operating. Bruker Vertex 70 with an MCT detector was used to collect diffuse reflectance infrared Fourier transform spectroscopy (DRIFTS). The sample was pretreated with Ar flow (30 mL/min) at 150 °C for 1 h, and the background was recorded after cooling to room temperature. The sample was then exposed to CO flow (30 ml/min) for 30 min. The Ar flow (30 mL/min) was introduced to remove physically adsorbed species, and the CO-DRIFTS spectrum was collected. For nitrobenzene-DRIFTS, 30 mL/min of Ar carrying the volatilized nitrobenzene was continuously introduced into the cell for saturated adsorption followed by Ar purge. Temperature programmed desorption of nitrobenzene (nitrobenzene-TPD) was conducted on a Thermo Scientific Lindberg Bule M instrument with connecting mass spectrometry (Thermostar). The sample was purged with Ar (30 mL/min) for 1 h at 150 °C and then cooled to room temperature. The sample was adsorbed with nitrobenzene for 3 h, and the remaining nitrobenzene was purged by Ar for another 3 h. Finally, the desorption of nitrobenzene was carried out by heating to 400 °C at a rate of 5 °C/min under Ar atmosphere. The signals were measured using mass spectrometry. The DRIFTS and TPD results were normalized.

Catalytic reaction

Nitrobenzene hydrogenation reactions were performed in a 50 mL stainless steel autoclave with a magnetic stirrer. In each reaction, 50 mg catalyst, 30 mL cyclohexane, 2.04 mL (20 mmol) nitrobenzene, and 2.94 mL (13 mmol) dodecane (used as internal standard) were transferred into the autoclave. Before reaction, the reactor was purged with N_2 several times in order to remove the air. The system was then raised to the target temperature and the vessel was pressurized by 3 MPa H_2. After the reaction, the

products were collected by centrifugation and analyzed by an Agilent 7890B gas chromatograph. Witout other treatment.

The stability of $PtPdCoCuNi/SiO_2$ catalyst was investigated by cycling for five times under the same conditions. The catalyst after each reaction run was recovered by centrifugation, then washed with ethanol and used for next run after drying without other treatment.

Computational method

All first-principles data were obtained using the density functional theory (DFT) method implemented in the Vienna Ab initio simulation package (VASP)[1, 2] and periodic slab models. The projector-augmented-wave (PAW)[3] method was employed, which is an all-electron DFT technique to present electron-ionic interactions. The electron exchange correlation was treated by the well-known generalized gradient approximation in the Perdew–Burke–Ernzerhof form (GGA-PBE)[4]. For the sake of providing an exact description of the magnetic properties, calculations of spin-polarization were carried out, which are also essential to the adsorption energy calculations. In order to ensure that the energy errors were within a reasonable range, an energy cutoff of 500 eV and the second order Methfessel-Paxton[5] electron smearing with $\sigma = 0.05$ eV were used. The vacuum layer between periodically repeated slabs was set as 10 Å to avoid interactions among slabs.

The adsorption energy (E_{ads}) of one nitrobenzene molecule is defined as $E_{ads} = E_{nitrobenzene/slab} - [E_{slab} + E_{nitrobenzene}]$, where $E_{nitrobenzene/slab}$ is the total energy of the slab with one nitrobenzene adsorption, E_{slab} is the total energy of the bare slab and $E_{nitrobenzene}$ is the total energy of a free nitrobenzene molecule in gas phase, and a more negative E_{ads} indicates a stronger adsorption.

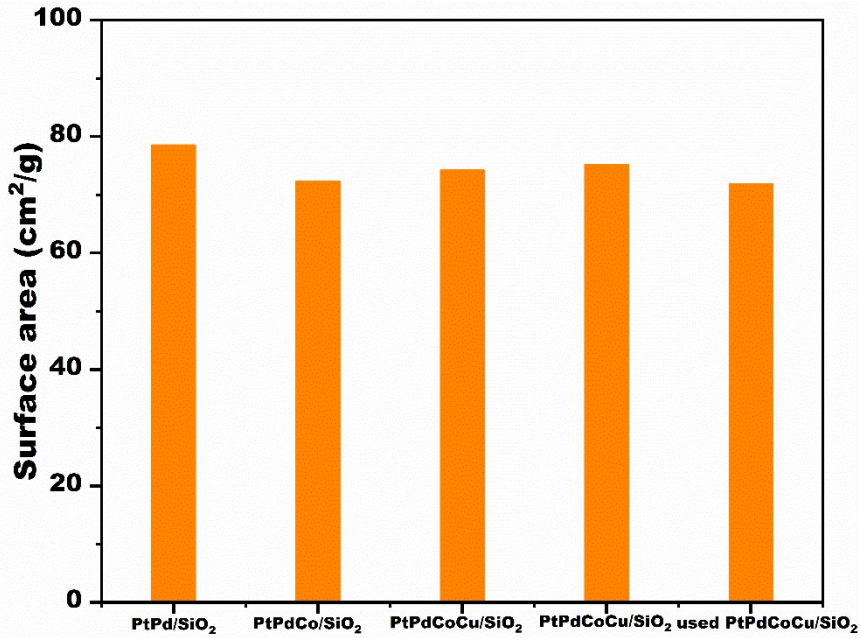

Fig. S1 BET surface area of $PtPd/SiO_2$, $PtPdCo/SiO_2$, $PtPdCoCu/SiO_2$, $PtPdCoCuNi/SiO_2$, and used $PtPdCoCuNi/SiO_2$ catalysts. These catalysts have the similar BET surface area.

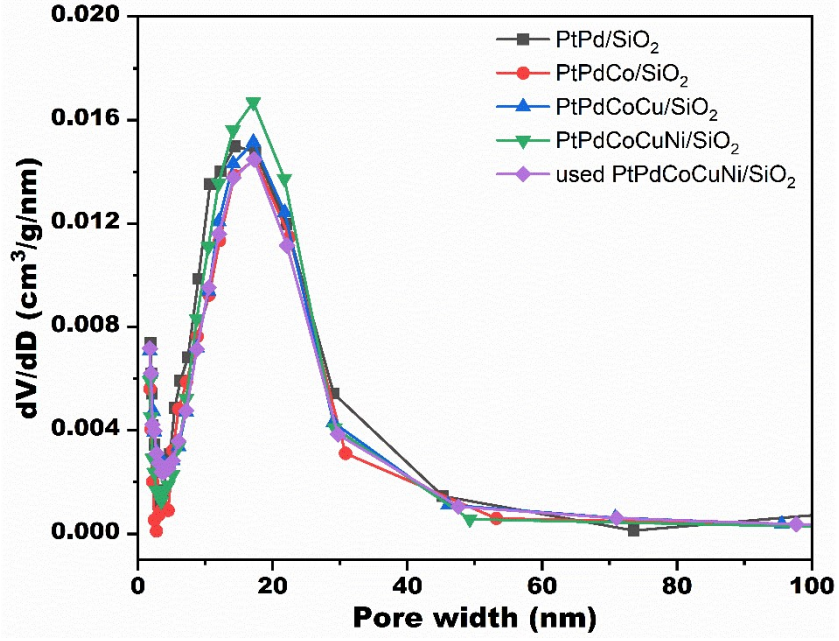

Fig. S2 Pore size distribution of $PtPd/SiO_2$, $PtPdCo/SiO_2$, $PtPdCoCu/SiO_2$, $PtPdCoCuNi/SiO_2$, and used $PtPdCoCuNi/SiO_2$ catalysts. There is no obvious difference in pore size distribution of these catalysts.

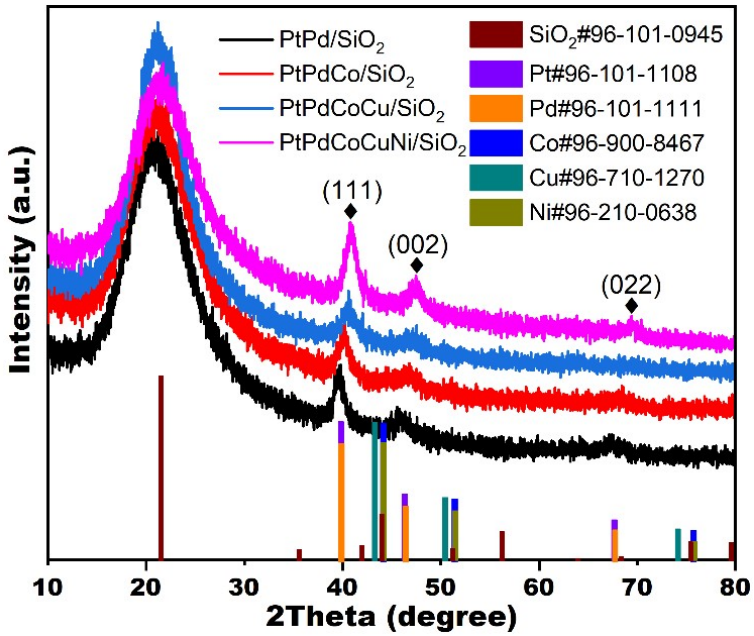

Fig. S3 XRD patterns of $PtPd/SiO_2$, $PtPdCo/SiO_2$, $PtPdCoCu/SiO_2$, and $PtPdCoCuNi/SiO_2$ catalysts. The observed peaks can be assigned to (111), (002), and (022) planes of polymetallic nanoparticles with the fcc structure. The diffraction peaks exhibit obvious shifts to higher angles with increasing the metal composition, which is due to lattice contraction caused by lattice distortion.

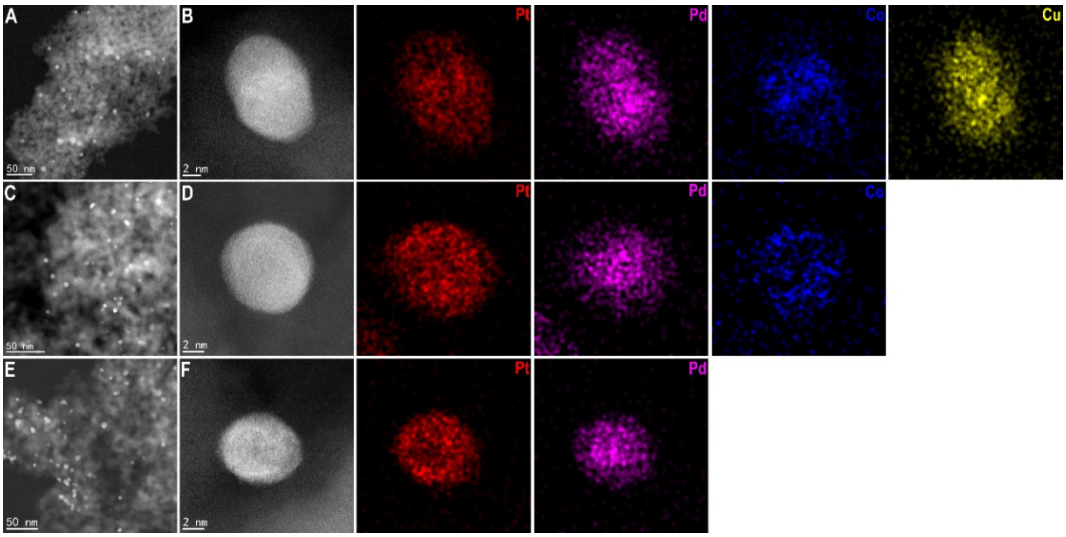

Fig. S4 (A) STEM-ADF image and (B) STEM-ADF image and corresponding elemental mapping of $PtPdCoCu/SiO_2$ catalyst; (C) STEM-ADF image and (D) STEM-ADF image and corresponding elemental mapping of $PtPdCo/SiO_2$ catalyst; (E) STEM image and (F) STEM image and corresponding elemental mapping of $PtPd/SiO_2$ catalyst. According to STEM-ADF images of $PtPdCoCu/SiO_2$, $PdPdCo/SiO_2$, and $PdPd/SiO_2$ catalysts, the nanoparticles with uniform morphology and size are evenly dispersed on SiO_2 support. The EDS elemental mappings show that the corresponding metal elements are distributed throughout the nanoparticles, indicating the formation of alloy nanoparticles.

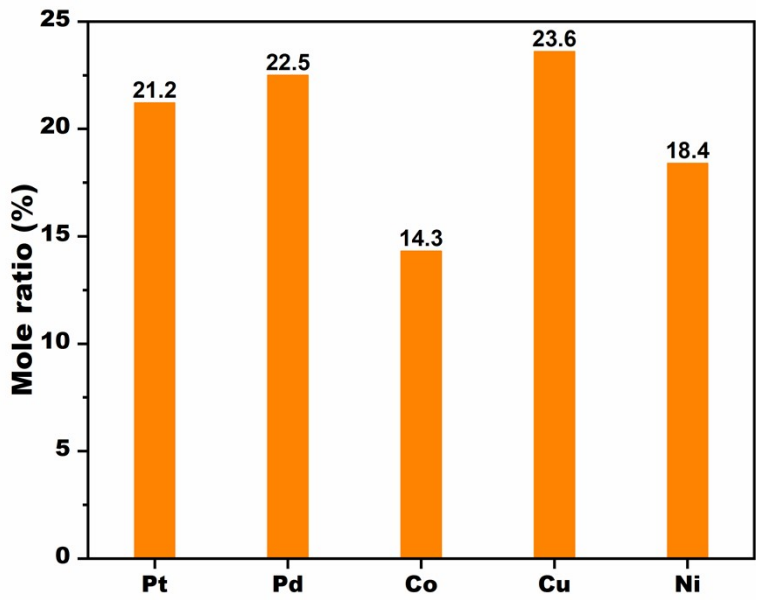

Fig. S5 Compositional distribution of quinary PtPdCoCuNi/SiO_2 catalyst based on ICP-AES. The total metal loading was measured to be about 1.66 wt% for PtPdCoCuNi/SiO_2 catalyst, which was very close to the theoretical loading (2.0 wt%).

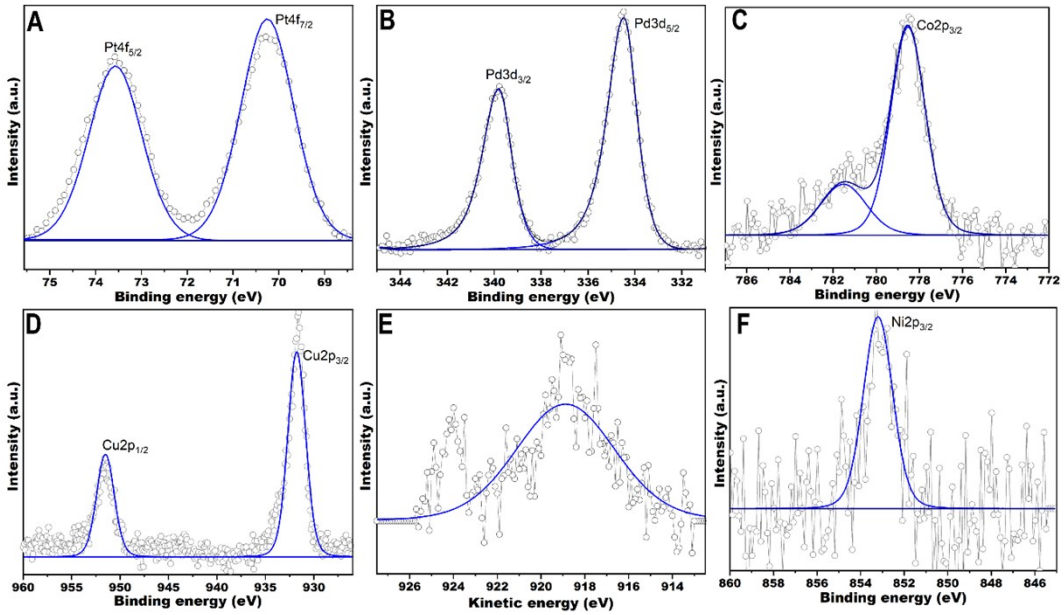

Fig. S6 XPS spectra of (A) Pt 4f, (B) Pd 3d, (C) Co 2p, (D) Cu 2p, (E) Cu LMM Auger, and (F) Ni 2p of PtPdCoCuNi/SiO_2 catalyst.

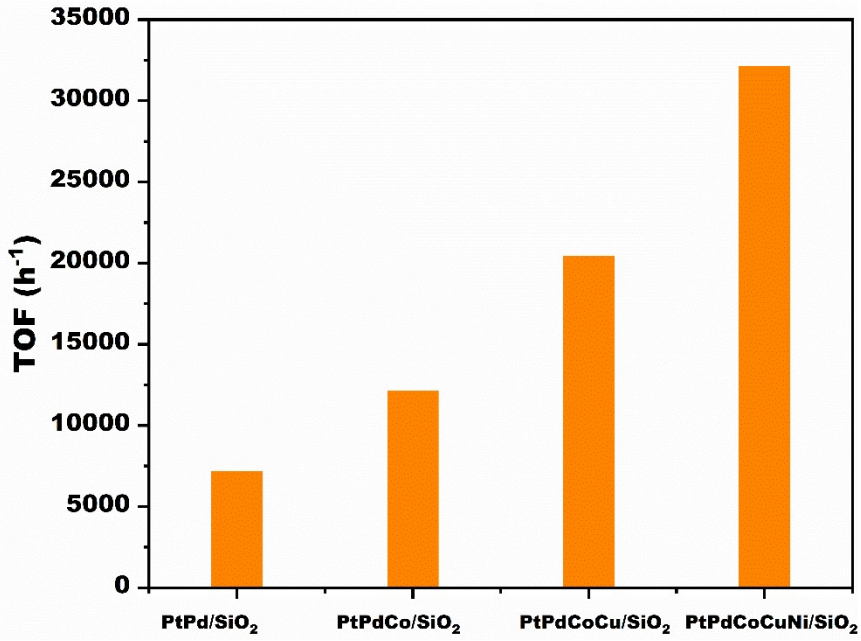

Fig. S7 The turnover frequency (TOF) of PtPd/SiO_2, PtPdCo/SiO_2, PtPdCoCu/SiO_2, and PtPdCoCuNi/SiO_2 catalysts. TOF was based on the amount of Pt and Pd.

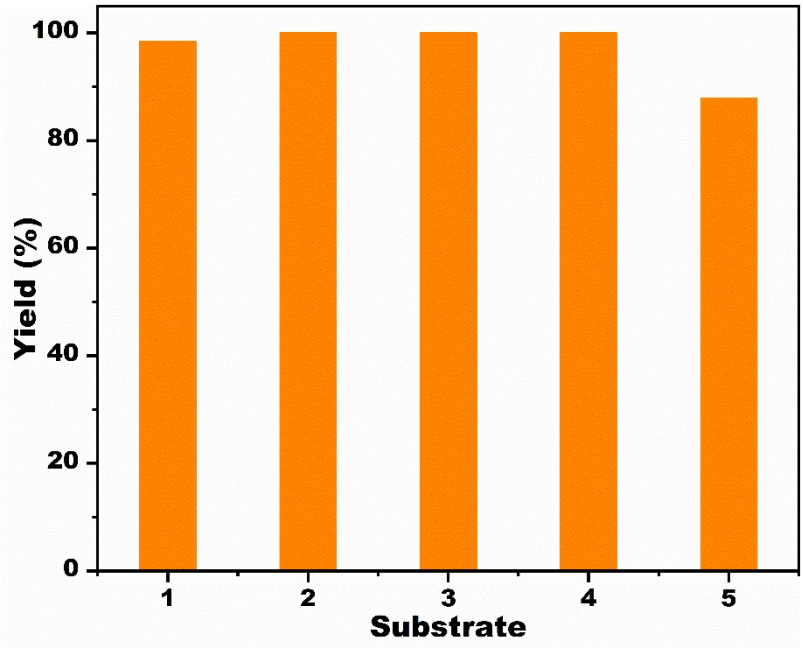

Fig. S8 Hydrogenation of various substituted nitroarenes over PtPdCoCuNi/SiO_2 catalyst. Reaction conditions: 50 mg catalyst, 600 rpm, 3 MPa H_2, 80 °C, 2 h, 30 mL alcohol, 5 mmol substrate. (1: 1-chloro-3-nitrobenzene, 2: 3-nitrotoluene, 3: 4-nitrophenol, 4: 4-nitrobenzyl alcohol, 5: 1-bromo-4-nitrobenzene)

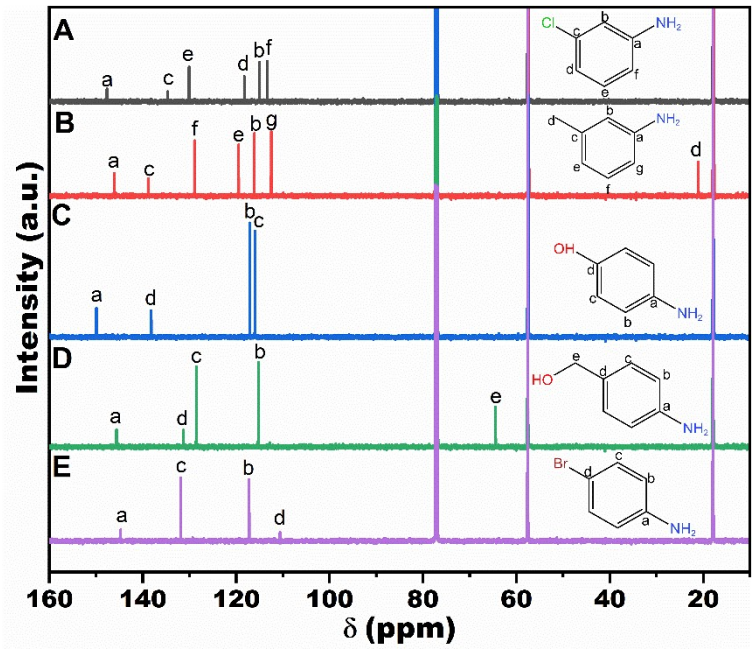

Fig. S9 ^{13}C NMR spectra of various substituted aromatic amines (A: m-chloroaniline, B: m-toluidine, C: p-aminophenol, D: p-aminobenzyl alcohol, E: 4-bromoaniline).

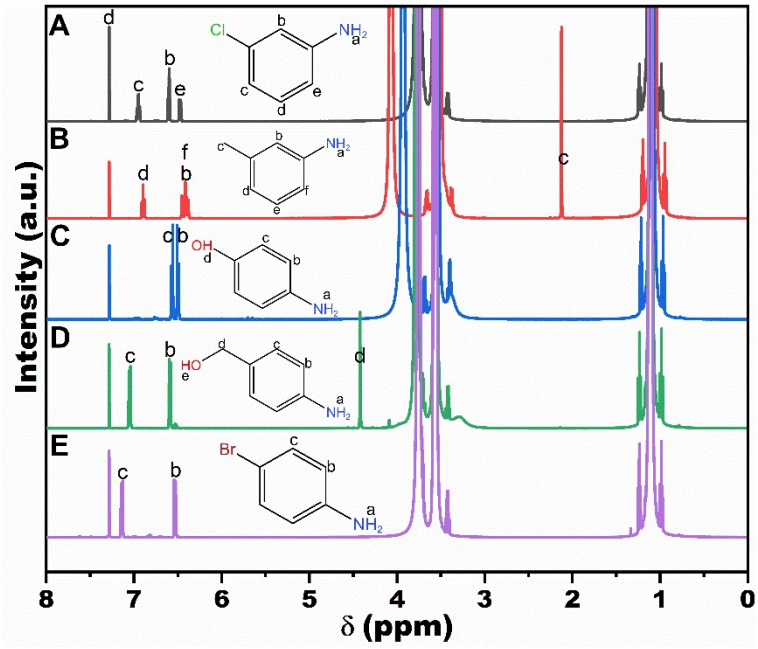

Fig. S10 ^{1}H NMR spectra of various substituted aromatic amines (A: m-chloroaniline, B: m-toluidine, C: p-aminophenol, D: p-aminobenzyl alcohol, E: 4-bromoaniline).

Table S1. Comparison of the turnover frequency of some most active Pt or Pd-based catalysts toward nitrobenzene hydrogenation.

Entry	Catalyst	Substrate mmol	T (°C)	H_2	TOF (h^{-1})	Ref.
1	PtCo nanoflower	0.5	25	1 bar	200	1
2	Pt-Ni nanodendrites	0.5	25	balloon	200	2
3	Pd/CeO_2	50.0	40	6 MPa	11411	3

4	PtCu nanosheets	1.0	25	0.1 MPa	1000	4
5	Pd/LDH	0.8	50	1 MPa	134	5
6	Pd@SiO_2	29.5	45	0.1 MPa	6209	6
7	Pd NSs	0.5	25	balloon	43	7
8	Pt/SiO_2	2.0	100	3.0 MPa	2196	8
9	Pd/SiO_2	2.0	100	3.0 MPa	10800	8
10	Pd/N@CNT	20.0	45	0.5 MPa	9000	9
11	PtPdCoCuNi/SiO_2	20.0	80	3.0 MPa	32170	This work
12	PtPdCoCuNi/SiO_2	20.0	50	3.0 MPa	12576	This work
13	PtPdCoCuNi/SiO_2	20.0	25	3.0 MPa	6479	This work

The TOF was based on the amount of Pt or Pd.

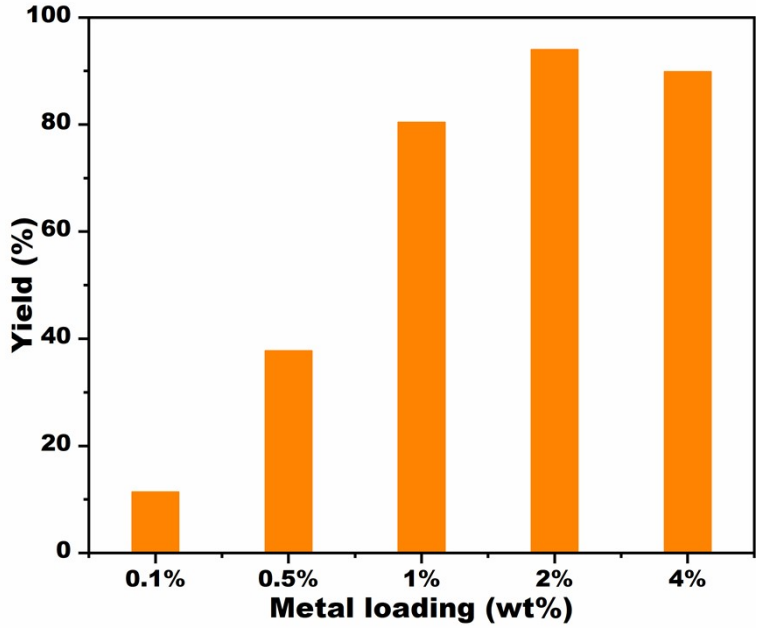

Fig. S11 Aniline yield over supported PtPdCoCuNi catalyst with different metal loading. Reaction conditions: 50 mg catalyst, 600 rpm, 3 MPa H_2, 80 °C, 2 h, 30 mL cyclohexane, 20 mmol nitrobenzene.

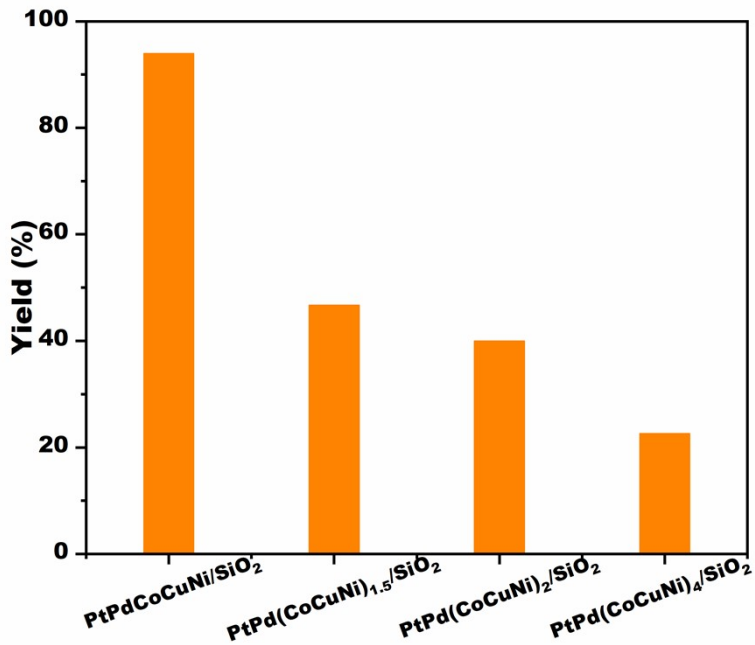

Fig. S12 Aniline yield over $PtPd(CoCuNi)_x/SiO_2$ (x = 1, 1.5, 2, and 4, x is the mole ratio of CoCuNi to PtPd) catalysts. Reaction conditions: 50 mg catalyst, 600 rpm, 3 MPa H_2, 80 °C, 2 h, 30 mL cyclohexane, 20 mmol nitrobenzene.

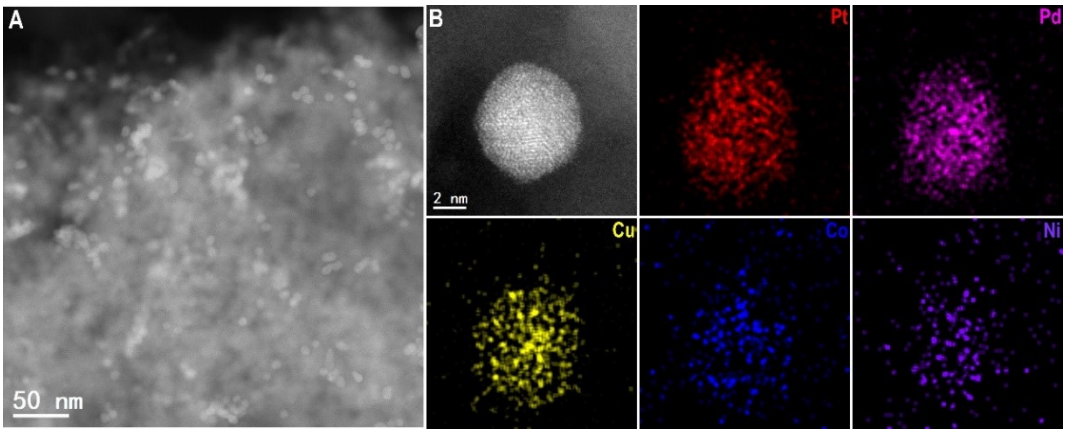

Fig. S13 (A) STEM-ADF image and (B) STEM-ADF image and corresponding EDS elemental mapping of used $PtPdCoCuNi/SiO_2$ catalyst.

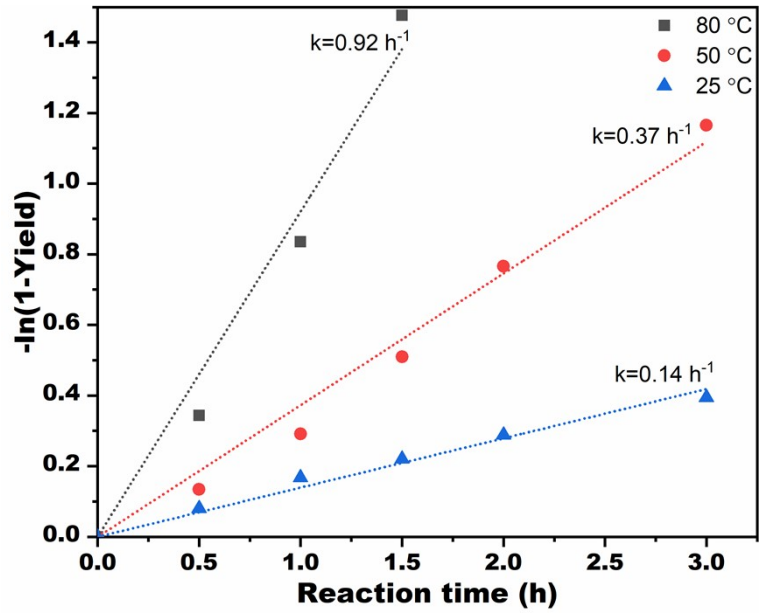

Fig. S14 First-order kinetic plots for nitrobenzene hydrogenation over $PtPdCoCuNi/SiO_2$ catalyst. Reaction conditions: 50 mg catalyst, 600 rpm, 3 MPa H_2, 30 mL cyclohexane, 20 mmol nitrobenzene.

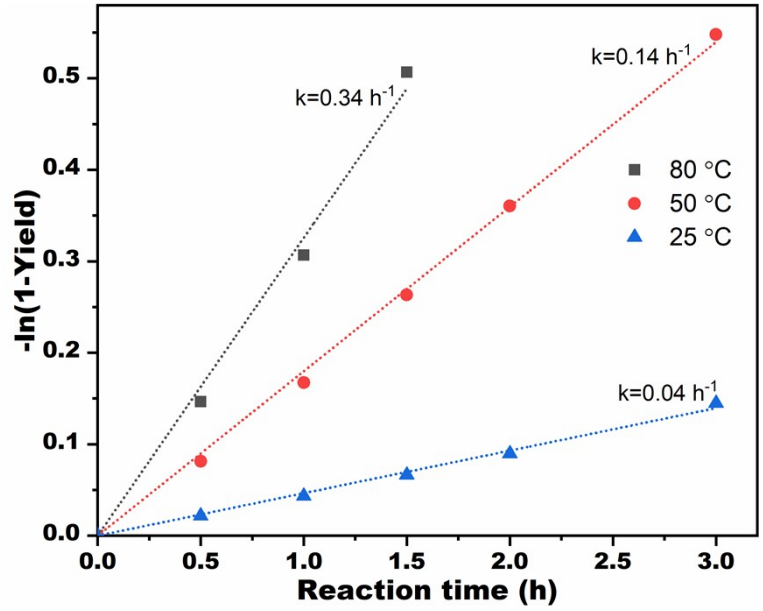

Fig. S15 First-order kinetic plots for nitrobenzene hydrogenation over $PtPd/SiO_2$ catalyst. Reaction conditions: 50 mg catalyst, 600 rpm, 3 MPa H_2, 30 mL cyclohexane, 20 mmol nitrobenzene.

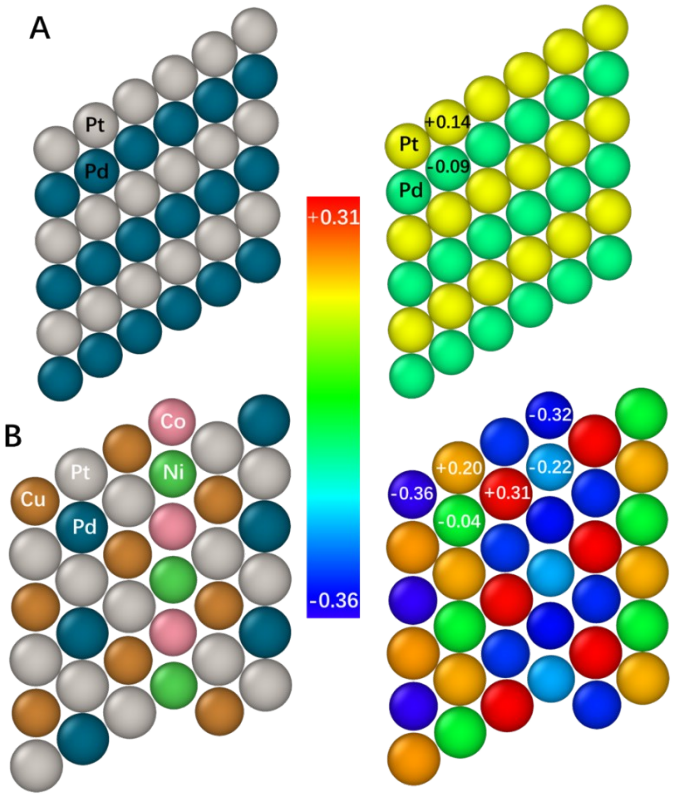

Fig. S16 Atomic arrangement and differential charge distributions of (A) PtPd and (B) PtPdCoCuNi alloy slabs.

References

1 G. Kresse and J. Furthmuller, *Comput. Mater. Sci.*, 1996, **6**, 15-50.

2 G. Kresse and J. Furthmüller, *Phys. Rev. B*, 1996, **54**, 11169-11186.

3 P. E. Blöchl, *Phys. Rev. B*, 1994, **50**, 17953-17979.

4 J. P. Perdew, K. Burke and M. Ernzerhof, *Phys. Rev. Lett.*, 1996, **77**, 3865-3868.

5 M. Methfessel and A. T. Paxton, *Phys. Rev. B*, 1989, **40**, 3616-3621.

6 H. Miao, S. Hu, K. Ma, L. Sun, F. Wu, H. Wang and H. Li, *Catal. Commun.*, 2018, **109**, 33–37.

7 W. Wang, D. Wang, X. Liu, Q. Peng and Y. Li, *Chem. Commun.*, 2013, **49**, 2903–2905.

8 X. Shi, X. Wang, X. Shang, X. Zou, W. Ding and X. Lu, *ChemCatChem*, 2017, **9**, 3743–3751.

9 L. Dai, Y. Zhao, Q. Qin, X. Zhao, C. Xu and N. Zheng, *ChemNanoMat*, 2016, **2**, 776–780.

10 J. Wang, C. Du, Q. Wei and W. Shen, *Energy Fuels*, 2021, **35**, 4358–4366.

11 Y. Hu, K. Tao, C. Wu, C. Zhou, H. Yin and S. Zhou, *J. Phys. Chem. C*, 2013, **117**, 8974–8982.

12 Z. Huang, S. Li, B. Xu, F. Yan, G. Yuan and H. Liu, *Small*, 2021, **17**, 2006624.

13 M. Tamura, K. Kon, A. Satsuma and K.-i. Shimizu, *ACS Catal.*, 2012, **2**, 1904–1909.

14 Z. He, B. Dong, W. Wang, G. Yang, Y. Cao, H. Wang, Y. Yang, Q. Wang, F. Peng and H. Yu, *ACS Catal.*, 2019, **9**, 2893–2901.